AD_____
(Leave blank)

Award Number:
W81XWH-07-1-0149

TITLE:
Exploiting a Molecular Gleason Grade for Prostate Cancer Therapy

PRINCIPAL INVESTIGATOR:
Peter S. Nelson, M.D.

CONTRACTING ORGANIZATION:
Fred Hutchinson Cancer Research Center
Seattle, WA 98109

REPORT DATE:
March 2009

TYPE OF REPORT:
Annual

PREPARED FOR: U.S. Army Medical Research and Materiel Command
Fort Detrick, Maryland 21702-5012

DISTRIBUTION STATEMENT:

X Approved for public release; distribution unlimited

Distribution limited to U.S. Government agencies only; report contains proprietary information

REPORT DOCUMENTATION PAGE

Form Approved
OMB No. 0704-0188

1. REPORT DATE *(DD-MM-YYYY)*	**2. REPORT TYPE**	**3. DATES COVERED** *(From - To)*
03/14/2009	Annual	02/15/2008-02/14/2009

4. TITLE AND SUBTITLE
Exploiting a Molecular Gleason Grade for Prostate Cancer Therapy

5a. CONTRACT NUMBER
W81XWH-07-1-0149

5b. GRANT NUMBER
PC060595

5c. PROGRAM ELEMENT NUMBER

6. AUTHOR(S)
Peter S. Nelson, M.D.

5d. PROJECT NUMBER

5e. TASK NUMBER

5f. WORK UNIT NUMBER

7. PERFORMING ORGANIZATION NAME(S) AND ADDRESS(ES)
Fred Hutchinson Cancer Research Center

1100 Fairview Ave N
PO Box 19024
J6-500
Seattle, WA 98109-1024

8. PERFORMING ORGANIZATION REPORT NUMBER

9. SPONSORING / MONITORING AGENCY NAME(S) AND ADDRESS(ES)
U.S. Army Medical Research
And Materiel Command
Fort Detrick, MD 21702-5012

10. SPONSOR/MONITOR'S ACRONYM(S)

11. SPONSOR/MONITOR'S REPORT NUMBER(S)

12. DISTRIBUTION / AVAILABILITY STATEMENT
Approved for public release; distribution unlimited

13. SUPPLEMENTARY NOTES

14. ABSTRACT
The Purpose of this proposal is to exploit a molecular correlate of the Gleason grading system for prostate carcinoma in order to: a) develop improved outcome predictors; and b) identify therapeutic strategies. During this project period we have evaluated in excess of 25 prostate cancer antigens by Western blot and tissue-based assays and identified 3 with detectable levels in the plasma. We also determined that developmental genes involved with invasive cellular behavior exhibit associations with clinical outcomes. While these results are important, the further exploitation of these findings is limited by the lack of specific antibodies suitable for tissue (IHC) and ELISA-based studies of protein localization and quantitation. Ongoing studies are focused on developing alternative strategies for protein quantitation in order to complete the proposal objectives.

15. SUBJECT TERMS

16. SECURITY CLASSIFICATION OF:			**17. LIMITATION OF ABSTRACT**	**18. NUMBER OF PAGES**	**19a. NAME OF RESPONSIBLE PERSON**
a. REPORT	**b. ABSTRACT**	**c. THIS PAGE**			USAMRMC
U	U	U	UU	18	**19b. TELEPHONE NUMBER** *(include area code)*

Table of Contents

Page

INTRODUCTION

This proposal is designed to exploit a molecular correlate of the Gleason grading system for prostate carcinoma in order to: *a)* develop improved outcome predictors; and *b)* identify therapeutic strategies targeted toward features unique to aggressive cancers. We hypothesized that the specific molecular features that underlie prostate cancer grades define the capacity for tumor cell invasion and dissemination (progression) and may represent unique diagnostic markers and targets for therapeutic intervention.

The aims of the proposal remain unchanged: Aim #1: To compare the power of molecular versus histological Gleason categories for outcome predictions in the context of PSA relapse and prostate cancer-specific mortality. Aim #2: Determine if grade-associated differences in prostate cancer protein expression are reflected by levels of cognate serum proteins. #3 Write final report. (Note the original Aim 3 involving animal studies of altering prostate cancer grade-associated functions was deleted due to recommendations by the reviewers).

Disease relevance: Through comprehensive studies of genome and gene expression alterations, it is clear that prostate cancers are profoundly heterogeneous, both at the molecular and clinical level. In this context, the successful completion of this proposal has the potential to greatly improve clinical decision making by improving the accuracy of predicting which cancers may best be 'treated' by observation rather than primary therapy, or defining those cancers that should have additional systemic therapy---in addition to local therapy---by virtue of their high malignant potential. Also in the context of clinical care, several of the key nodes distinguishing low grade from high-grade cancer feature metabolic components that currently can be targeted by FDA-approved drugs originally designed for the treatment of diseases other than neoplasia (e.g. MAOA inhibitors).

BODY

The following summarizes the technical objectives for the proposal and the work accomplished during the 12-month interval between the Year 1 Progress Report (02/08) and the present Year 2 Progress Report (02/09). Work done during Year 1 (02/07-02/08) and reported last year is included in parentheses (..) as a frame of reference.

D.1.Technical objective 1: To compare the predictive power of molecular versus histological Gleason categories for outcome predictions in the context of PSA relapse and prostate cancer-specific mortality. (Months 1-24).

Objective 1a. *Antibody acquisition and evaluation*.

Task 1: purchase antibodies recognizing grade-determinant proteins (months 1-12).

(Year 1: To date, we have purchased (or acquired) antibodies recognizing; TMPRSS2, MAOA, DAD1, ERG, Jagged, p63, AMACR, MUC1, FLNA, ALSCR2, CCNG2, FLH2, GSTMU1, PC4, RSK2, and SMS. The majority of these have previously been used in immunohistochemical studies, though not in prostate cancer.)

Year 2: We have purchased an additional 25 antibodies for the evaluation of prostate cancer associated gene/protein expression: Postn, Arf1, Arf2, Cltc, Lamc2, Msn, Nrp1, Ppp1cc, Psma7, Tpm3, Tuba1a, Tuba1b, Tuba4a, AZGP1, PTPRF, ADAM7, ADAM9, ADAMTS5, ALCAM, CXCL12, EFNA1, HSPD1, JAG2, NOTCH3, and STOML2.

Task 2: evaluate each antibody using a semi-quantitative immunoblot (months 1-12).

(Year 1: We performed semi-quantitative immunoblots for approximately 1/2 of these antibodies with the specific intent of demonstrating a specific band. However, we have found that this approach is not definitive, and does not provide additional data in our hands due to the profound heterogeneity in the tissue, and highly variable expression in cell lines.)

Year 2: We performed semi-quantitative immunoblots for 25 additional antibodies (see Task 1 above for Year 2) recognizing that despite the limitations of the approach, when moving forward to tissue staining, it is important to have an assessment of antibody specificity when interpreting immunostains---e.g. avoid a false-positive signal. While very few of these commercial antibodies provide a single band of expected protein size, several resulted in quite promising distinction between benign and cancerous prostate (*Figure 1*, Below Left, PTPRF shows elevated expression in prostate and breast carcinoma, *Figure 2*, Right, JAG2 shows elevated expression in prostate cancer and in several prostate cancer cell lines, and conditioned medium from these lines, indicating protein secretion), and several also detected an appropriate protein in serum from tumor bearing xenografts (see *Figure 3*, below).

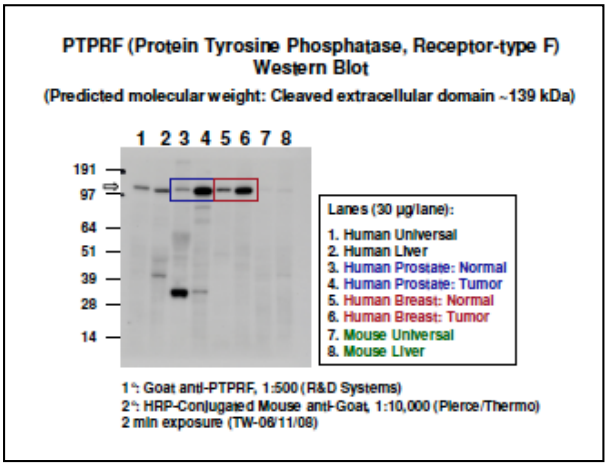

Figure 1. Elevated expression of PTPRF protein in prostate cancer tissue.

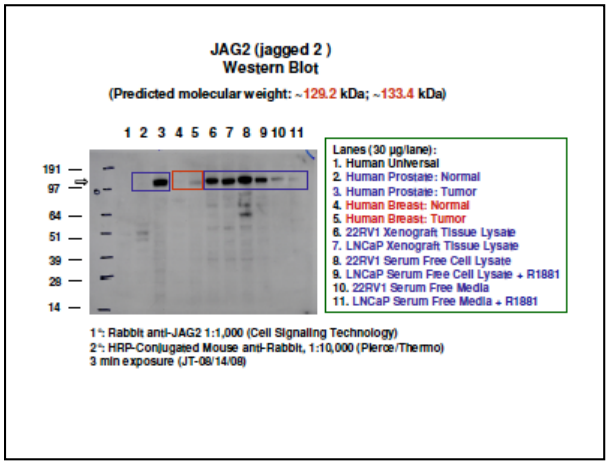

Figure 2. Elevated expression of JAG2 protein in prostate cancer tissue.

Task 3: optimize IHC staining using a fixation TMA, antibody dilutions and antibody retrieval methods (months 1-12).

(Year 1: We have optimized titering and conditions for the following antibodies against a small panel of benign and neoplastic prostate cases: TMPRSS2, MAOA, DAD1, ERG, Jagged, p63, AMACR, MUC1, FLNA, ALSCR2, CCNG2, FLH2, GSTMU1, PC4, RSK2, and SMS—see reportable outcomes, Datta et al (2007).

Year 2: We have continued optimization of antibody immunostaining for additional antibodies associating with grade/prostate cancer outcome. These have included ABP280L, ITGAS, PSA, MIB1, Muc1, Jagged1, AMACR, CDK7, MTA1 and SKC4A1AP.

Objective 1b. *IHC analysis/confirmation of protein expression and Gleason pattern*

Task 4: compare protein expression patterns relative to transcript measures by microarray (months 12-16).

(Year 1: We have initiated these studies. We have re-organized grade-defining genes present on our original microarray studies into a format that can be directly compared to protein expression levels determined by IHC. We are now in the process of quantitating the protein expression across Gleason-appropriate prostate cancer cases, and will import the data directly for compari-

son. We have completed a thorough analysis of the expression of TMPRSS2, a grade-associated protein. *Figure 1* demonstrates TMPRSS2 expression in benign and cancer epithelium and shows mislocalization of TMPRSS2 in cancer cells. *Figure 2* demonstrates Gleason Grade-associated TMPRSS2 expression.)

Year 2: We are continuing these studies. To date, very few of the antibodies have yielded consistent transcript and protein correlations. TMPRSS2 is an exception where we found clear correlations between transcript and protein upregulation in prostate cancer that also associated with Gleason grade (see Reportable Outcomes from Year 1, Lucas et al). A component of this discordance is likely due to the protein localization in different cellular compartments (e.g. membrane vs nucleus). Another component of this discordance may lie in the lack of antibody specificity. A third component of this discordance may simply reflect lack of clear concordance between transcript and protein levels in cells/tissues.

Objective 1c. *IHC analysis of prostate cancer cohorts with outcomes reflected by PSA relapse and mortality*.

Task 5: Stain and read Gelman TMAs: 20 antibodies (months 16-22)

Year 2: We completed 'outcomes' studies of the TMPRSS2 antibody on the Gelman TMA and found no correlation with relapse that was independent of Gleason Grade (see Reportable Outcomes for Year 1, Lucas et al). In the process of conducting these studies, we determined that this TMA is not optimal for completing all of the planned studies due to the limited numbers of these arrays that will actually be available. Thus, we have initiated the construction additional TMAs with outcomes. We have developed a network of collaborating institutions (5 different sites) that will each construct outcomes TMAs suitable for cross-comparison of IHC results in the context of outcomes associations. We have identified 200 cases within our Center that will be used and construction of this TMA has commenced with planned completion by 6/09. The planned IHC studies for Task 5 will commence at that time. We have constructed a 50 case outcomes TMA and have used this resource to evaluate outcomes of 4 markers to date. (see Task 7).

Task 6: Stain and read Stanford TMAs: 20 antibodies (months 16-22). The construction of the Stanford TMA was delayed due to logistics of acquiring all sample blocks by Dr. Stanford's group. These blocks have now been collected and the construction of this TMA has commenced with an anticipated completion date of 07/09.

Year 2:

Task 7: Determine statistical associations with outcomes (months 22-24). We found no independent correlations with TMPRSS2 expression and clinical outcomes using the original Gelman TMA. We have completed a study of 4 grade/outcome-associated antibodies (ITGAS, PSA, MIB1, MTA1) and found no correlations with outcomes using the 50-case outcomes TMA. These will be repeated using the 200 case outcomes TMAs and the Stanford TMA.

In a companion study that involved assessing molecular correlates of prostate development, we identified genes associated with the branching morphogenesis/invasive component of development and features of prostate carcinoma. Several of these genes were Gleason grade-associated genes. We examined existing prostate cancer datasets with annotated clinical outcomes, and determined that several of these developmental genes associated with prostate cancer relapse following primary therapy (see Figure 4, in the appended manuscript provided in ***Reportable Outcomes***, Pritchard *et al*). This study provides additional candidates to evaluate in the context of grade/outcome markers for prostate cancer that is the focus of the present application, and we are currently obtaining antibodies for verification studies based on tissue protein expression.

Task 8: Refine antibody/protein list to minimal redundant set. (months 22-24)

Year 2: This task is pending the completion of the TMA studies above in Tasks 6-7.

D.2. Technical objective 2: *Determine if grade-associated differences in prostate cancer protein expression are reflected by levels of serum proteins* (months 3-36).

Objective 2a. *Western Analysis for Antibody Q/C.*

Task 9: prepare Western blots of serum proteins (months 3-6).

(Year 1: We have acquired a panel of (anonymized) human serum protein samples that span a spectrum of a) absence of prostate cancer—biopsy proven; b) low grade prostate cancer; c) high grade prostate cancer; d) metastatic prostate cancer. The quality of the samples has been verified using Western analysis for abundant and low abundant proteins.

Task 10: determine specificity of immunoreactivity and semi-quantitation (months 7-12).

(Year 1: We have completed Western analysis (blots) for 12 proteins/antibodies. Of these, four antibodies produced patterns indicating poor specificity, with multiple bands present. Of the remaining 8, three did not provide satisfactory detection, and these are being re-evaluated, or another antibody source is being evaluated. The remaining five demonstrating good specificity and we are scaling up a larger sample set to assess overall cancer/benign/grade evaluation. One protein, osteopontin, is capable of distinguishing metastatic cancer, but not early stage cancer, relative to individuals without cancer.)

Year 2: We have completed the serum-based analysis of an additional 25 antibodies recognizing prostate cancer antigens (see Objective 1a, Task 1, Year 2). Of these, 10 recognized an appropriate band in conditioned medium from prostate cells and 3 recognized an appropriate band in the plasma of mice bearing prostate tumors (see *Figure 3*). Note, we have opted to use a stepwise approach for evaluating tumor-associated plasma proteins to save valuable human plasma. (The murine plasma samples were available from other ongoing studies and thus were not a cost to this project). The next phase will involve the direct evaluation of these candidates in human samples by Western blot and ELISA.

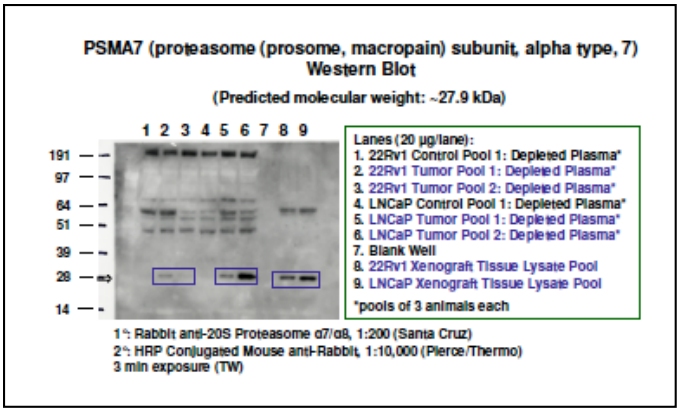

Figure 3. Expression of PSMA7 in the plasma of mice bearing prostate cancer xenografts (boxes). Note, absence of PSMA7 in serum of control mice (lanes 1 and 4).

Objective 2b. *ELISA*

Task 11: Prepare assay plates (months 6-10).

(Year 1: We have prepared ELISA plates for three antibodies combinations to date. Data for our studies of osteopontin are shown in Figure 1. We have established a system to avoid non-specific detection for these proteins. For the remainder of candidates, we are attempting to identify a second antibody as most ELISAs rely on two antibodies for specificity. If we are unable to identify a second antibody, we will proceed with a capture-ELISA or move toward other novel approaches such as SISCAPA (mass spectrometry-based assay—see task 16)).

Year 2: We have been unable to identify suitable secondary antibodies for the development of sandwich ELISAs for the candidate protein biomarkers (with the exception of osteopontin). The capture ELISAs have not been of sufficient sensitivity or specificity to detect protein levels. We are continuing to evaluate new ELISAs developed by commercial manufacturers to our can-

didate proteins, and we have initiated the development of new antibodies with a collaborator, Dr. Brad Nelson, at the University of British Columbia. We will evaluate these antibodies for sensitivity/specificity as they become available early in Year 3.

Task 12: Run q/c with recombinant protein standards. (months 10-11).

(Year 1: For two proteins, we have run q/c for two proteins and these have passed our metrics.)

Year 2: This has proven to be a significant challenge. We have run q/c for additional proteins and no ELISAs have passed q/c metrics. For this reason, we have opted to develop new antibodies as described above for Task 11, and we have moved forward with SISCAPA analyses (see Task 16). We have also initiated studies using single-antibody assays by the Luminex (bead-based) system.

Task 13: Analyze control and disease serum samples by ELISA (months 10-14).

(Year 1: We have recently run serum samples representing low grade and high-grade cancer as well as benign and metastasis. Data analysis is in progress.)

Year 2: We completed the sample analysis for Osteopontin and a manuscript detailing these results is in preparation (note, details of these results were shown in the Year 2 progress report).

Task 14: Repeat Tasks 10-13 for two additional proteins (months 14-24)-pending

Year 2: Due to difficulties obtaining two high-quality antibodies/candidate protein (required for capture ELISAs), we have yet to develop ELISAs for the other promising protein candidates (e.g. PSMA7-Figure 3). We are currently evaluating the Luminex system for the utilization of single-antibodies and continue to assess commercial inventories of new ELISAs being marketed. We have also begun studies using SISCAPA (see Objective 2c, below).

Task 15: Repeat Tasks 10-13 for two additional proteins (months 24-34)-pending

Objective 2c. *SISCAPA*

Task 16: Explore the utility of SISCAPA (Stable Isotope Capture by Anti-Peptide Antibodies) as an alternative (and improvement) to ELISA-based assays. (months 30-35).

Year 2: Due to the challenges we have observed in obtaining multiple high-quality (specific) antibody reagents, we have started evaluating the SISCAPA approach for protein quantitation. This involves the development of mass spectrometry peptide sprectra for the candidate proteins. We have now identified highly specific spectra for peptides corresponding to 16 of the 25 candidate proteins described in Specific Aim 1a, Year 2. We are currently determining if these peptides can be observed by mass spectrometry in the serum of tumor-bearing hosts.

D.3. Technical objective 3: Final Report: Complete data analyses, compile accomplishments and reportable outcomes and write final project report (Months 35-36)-pending.

KEY RESEARCH ACCOMPLISHMENTS (Year 2)

- We completed the acquisition and preliminary analysis of 25 additional antibodies that recognize a subset of Gleason Grade-associated molecular changes found in human prostate cancer. Several were capable of distinguishing benign from malignant prostate and 3 recognized a protein of appropriate size in the plasma of tumor-bearing mice. The development of quantitative detection methods for these proteins is in progress (e.g. ELISA, SISCAPA).
- We integrated a study of prostate development and prostate carcinoma to identify a cohort of prostate cancer genes that associate with clinical outcomes, a subset of which include Gleason-associated genes (see Reportable Outcomes). Characterization of protein-based quantitation is in progress.

- We assembled the requisite tissue resources to construct tissue microarrays (TMAs) of suitable quality and quantity (number of tissue sections to allow for the planned antibody assays) to enable outcome studies of candidate Gleason grade-associated proteins.

REPORTABLE OUTCOMES

Year 1:

Datta MW, True LD, Nelson PS, Amin MB. The role of tissue microarrays in prostate cancer biomarker discovery. (2007) *Adv Anat Pathol*.Nov;14(6):408-18.

Lucas J, True L, Hawley S, Matsumura M, Morrissey C, Vessella R, Nelson P. (2008) The androgen-regulated type II serine protease TMPRSS2 is differentially expressed and mislocalized in prostate adenocarcinoma. *J Pathol*. 215:118-125.

Year 2:

Pritchard C, Mecham B, Dumpit R, Coleman I, Bhattacharjee M, Chen Q, Sikes RA, Nelson PS. (2009). Conserved gene expression programs integrate mammalian prostate development and tumorigenesis. Cancer Res. 2009 Mar 1;69(5):1739-47.

CONCLUSIONS

We have demonstrated that cancer and grade-associated mRNA abundance levels are associated with corresponding protein alterations for a subset (but not all) of candidates. The major limitation to our studies at this juncture is the lack of availability of high quality antibody reagents that are essential for developing a protein-based (IHC and serum) correlate to our transcript studies of Gleason grade. This is not unique to our studies, as high-quality antibody reagents are a limiting factor for many studies of protein correlates of gene expression in cells and tissues. However, we have several promising candidates based on our studies accomplished to date with available antibodies and have embarked on several alternative strategies that we anticipate will allow for the completion of the project. These include: (i) development of bead-based protein assays that allow for the use of a single, rather than 2, antibodies; (ii) development of SISCAPA-based approaches for mass spectrometry-based protein quantitation; (iii) development of new antibodies.

REFERENCES

None

APPENDICES

Manuscript: Pritchard C, Mecham B, Dumpit R, Coleman I, Bhattacharjee M, Chen Q, Sikes RA, Nelson PS. (2009). Conserved gene expression programs integrate mammalian prostate development and tumorigenesis. Cancer Res. 2009 Mar 1;69(5):1739-47.

Conserved Gene Expression Programs Integrate Mammalian Prostate Development and Tumorigenesis

Colin Pritchard,[1,4] Brig Mecham,[1,3] Ruth Dumpit,[1] Ilsa Coleman,[1] Madhuchhanda Bhattacharjee,[5] Qian Chen,[6] Robert A. Sikes,[6] and Peter S. Nelson[1,2,3,4]

Divisions of [1]Human Biology and [2]Clinical Research, Fred Hutchinson Cancer Research Center; Departments of [3]Genome Sciences and [4]Pathology, University of Washington, Seattle, Washington; [5]Department of Biological Sciences, University of Delaware, Newark, Delaware; and [6]School of Mathematics and Statistics, Mathematical Institute, University of St. Andrews, St. Andrews, Fife, United Kingdom

Abstract

Studies centered at the intersection of embryogenesis and carcinogenesis have identified striking parallels involving signaling pathways that modulate both developmental and neoplastic processes. In the prostate, reciprocal interactions between epithelium and stroma are known to influence neoplasia and also exert morphogenic effects via the urogenital sinus mesenchyme. In this study, we sought to determine molecular relationships between aspects of normal prostate development and prostate carcinogenesis. We first characterized the gene expression program associated with key points of murine prostate organogenesis spanning the initial *in utero* induction of prostate budding through maturity. We identified a highly reproducible temporal program of gene expression that partitioned according to the broad developmental stages of prostate induction, branching morphogenesis, and secretory differentiation. Comparisons of gene expression profiles of murine prostate cancers arising in the context of genetically engineered alterations in the *Pten* tumor suppressor and *Myc* oncogene identified significant associations between the profile of branching morphogenesis and both cancer models. Further, the expression of genes comprising the branching morphogenesis program, such as *PRDX4, SLC43A1*, and *DNMT3A*, was significantly altered in human neoplastic prostate epithelium. These results indicate that components of normal developmental processes are active in prostate neoplasia and provide further rationale for exploiting molecular features of organogenesis to understand cancer phenotypes. [Cancer Res 2009;69(5):1739–47]

Introduction

Studies involving normal developmental processes have revealed important parallels with carcinogenesis that involve key signaling mechanisms controlling the three-dimensional growth and organization of tissues (1, 2). Organogenesis is a complex process involving proliferation, pattern specification, and cellular differentiation orchestrated by an evolving transcriptional program (3). Many highly conserved pathways instrumental in dictating ordered organ and organismal morphogenesis, originally defined in model organisms such as *Drosophila melanogaster* and *Caenorhabditis elegans*, have been found to be altered in human cancers. Examples include networks involving Wnt/adenomatous polyposis coli/catenins, Notch/Delta/Jagged, fibroblast growth factor, epidermal growth factor, transforming growth factor β (TGFβ)/Smad, and Hedgehog/Patched/Smoothened. Importantly, information transmitted via pathways controlled by these molecular interactions dictates cellular behaviors beyond mitogenic responses to include positional sense, differentiation, invasion, motility, the production of matrix components, and synthesis of autocrine and paracrine signaling molecules.

Key features of normal prostate organogenesis involve characteristics that are also hallmarks of prostate neoplasia, including a dependence on hormonal signaling, severing of cell-cell contacts, invasion of epithelium into the organ microenvironment, cell migration, reestablishment of cell contacts, and the development of new blood vessel networks (4). The prostate gland is an endodermal derivative of the hindgut first formed in late fetal life when androgen produced by the testis induces urogenital sinus (UGS) epithelial invasion into the mesodermally derived UGS mesenchyme (5). The vast majority of work detailing prostate developmental processes has involved rodents in which the first prostate buds are visible at day 17 of embryogenesis. Branching morphogenesis shortly follows this inductive phase and proceeds through the first 15 days of postnatal life (6). Androgen levels steeply rise at puberty (25–30 days postnatal in the mouse), resulting in prostate growth and terminal secretory differentiation that is complete by ~45 days postnatal. Thus, the major events of mouse prostate development can be summarized in three broad steps that comprise prostate induction, branching morphogenesis, and secretory differentiation.

To date, the fundamental molecular processes mediating the malignant phenotypes of prostate cancer cells remain poorly defined. Because only limited temporal information can be gained from studies of any discrete focus of malignancy, we reasoned that systematically evaluating normal cellular processes that share features with prostate carcinogenesis may provide insights into additional networks, pathways, or individual molecular interactions that contribute to neoplastic growth. Prostate organogenesis and carcinogenesis both exhibit a dependence on androgenic hormones, and each is influenced by a complex cross-talk of paracrine factors operating between epithelium and stroma (mesenchyme; ref. 5). Further, alterations in key developmental signaling nodes, such as the Sonic Hedgehog and Notch networks, exhibit reproducible alterations in prostate carcinomas (7–9). Based on these findings, we sought to determine the relationships between the global genetic programs associated with the course of prostate organogenesis and those found to be influenced by oncogenic pathways leading to invasive cancer. Herein, we detail

Note: Supplementary data for this article are available at Cancer Research Online (http://cancerres.aacrjournals.org/).

Requests for reprints: Peter S. Nelson, Division of Human Biology, Fred Hutchinson Cancer Research Center, Mailstop D4-100, 1100 Fairview Avenue, Seattle, WA 98109-1024. Phone: 206-667-3377; Fax: 206-667-2917; E-mail: pnelson@fhcrc.org.

doi:10.1158/0008-5472.CAN-07-6817

the characterization of transcriptional profiles corresponding to intervals of normal prostate organogenesis, define their relationships to genetically engineered mouse models of prostate carcinoma, and investigate associations with human prostate cancer phenotypes.

Materials and Methods

Mouse prostate tissue dissection, RNA isolation, and RNA amplification. All mouse studies were performed in accordance with Institutional Animal Care and Use Committee–approved protocols. Whole male UGS (E14.5, E15.5, E16.5, E17.5, and E18.5) or separated prostate lobes (P7, P30, and P90) were dissected from C57BL6/J mice and snap frozen in liquid nitrogen. For each biological replication, we pooled 3 to 10 mice representing one or two litters. RNA from pools of UGS or specific prostate lobes (vp, ap, and dlp) was prepared using the Qiagen RNeasy Mini kit. We included an on-column DNaseI treatment to remove contaminating DNA. Before RNA amplification, we combined equal quantities of RNA from vp, ap, and dlp for the postnatal prostate samples. We amplified 1 μg of total RNA from each sample through one round using the Arcturus RiboAmp kit. For the E14.5 UGS reference sample, a second round of amplification was done to provide enough RNA for all microarrays. Quantitative reverse transcription-PCR (RT-PCR) showed no significant difference in the relative expression of two genes (*Plzf* and *Pdgfd*) between unamplified and amplified RNA.

Microarray analyses. cDNA microarrays enhanced for genes expressed in the developing mouse prostate were prepared as previously described (see Supplementary Data; ref. 10). The *Pten*-null prostate cancer data were generated in our laboratory and previously published (11). The *Myc*-transgenic prostate data were obtained online[7] (12). Based on UniGene mapping, 3,641 unique genes were shared between the MPEDB and U74Av2 microarrays. Of these, 3,593 were in common with the 7,993 genes used in the time course data. Significance analysis of microarrays software was used to identify differentially expressed genes across prostate development or between cancer and normal samples (13). Complete linkage hierarchical clustering was performed using Cluster 3.0 software (Eisen Lab) without weighting.

Principal component analysis (PCA) was performed using R. Expression values for each of the 7,993 genes were first centered to mean zero across the developmental time points spanning E15.5-P90. We performed PCA for all 7,993 mean-centered genes. The percent temporal variance captured by each of the first five temporal PCs was 29.8%, 16.3%, 8.8%, 7.6%, and 5.0%, with 100% of the variance captured by the first 41 PCs. To project the mouse prostate cancer models onto the development space, we implemented PCA on single-channel expression values for the mouse prostate development data and followed the methods described by Kho and colleagues (14).

Gene Ontology analysis. Functional analysis of the genes was carried out using a Bayesian integrated analysis (see Supplementary Data for detailed methods). From the Gene Ontology (GO) database, we obtained data on 208 biological processes, 64 cellular components, and 151 molecular functions. These were selected from levels 2 to 6 of the GO hierarchy that were represented by >10 distinct genes on the array to enable robust statistical analysis.

Analyses of human prostate cancer gene expression and outcomes. The human orthologs for the 91 unique branching morphogenesis Genbank identifiers were identified using the HomoloGene database at the National Center for Biotechnology Information and mapped to each of three independent prostate cancer data sets (see Supplementary Data). For each gene, expression differences between normal and cancer were assessed by paired, two-sample t test of $\log_2$-transformed signal values. To evaluate the power for branching morphogenesis genes to predict prostate tumor behavior, we evaluated human prostate cancer gene expression data sets with attendant clinical outcomes (see Supplementary Data). Logistic regression was then used to measure the association between prostate-specific antigen (PSA) relapse and gene expression levels. We selected the genes associated with recurrent disease at the $P = 0.05$ level and used them to classify the tumor samples into two groups with k-means clustering (see Supplementary Data for methods). The difference in disease-free survival, defined as no PSA relapse >0.1 in any follow-up time point, for the two groups was quantified using the survDiff function in R.

[7] http://doe-mbi.ucla.edu/myc_driven_prostate_cancer/

Results

Patterns of gene expression associate with stages of prostate development: prostate induction, branching morphogenesis, and secretory differentiation. The major events of mouse prostate development can be summarized in three steps: (*a*) prostate induction at E17.5, (*b*) branching morphogenesis at E18.5 through postnatal day 15, and (*c*) secretory differentiation at postnatal days 25 to 45. To characterize the transcriptional program associating with these events, we profiled gene expression in the prostate or prostate precursor tissues at seven time points corresponding to key stages of prostate organogenesis: embryonic days E15.5, E16.5, E17.5, and E18.5 and postnatal days P7, P30, and P90 (Fig. 1). We generated three independent biological samples for each time point and each sample was hybridized in a replicate design to a cDNA microarray designed to assess gene expression in the mouse prostate gland (10, 15). To make the time points directly comparable, a common reference RNA consisting of E14.5 male UGS was included. Comparing transcript levels derived from different developmental stages back to E14.5 reflects the unfolding program of prostate development in relationship to the most undifferentiated state. Overall, 70% of the expressed genes (5,586 unique transcripts) were significantly changed over the time course [false discovery rate (FDR) < 1%]. Because of the large number of replicates ($n = 6$ per time point), we were able to statistically detect small changes in gene expression but chose to arbitrarily confine further analyses to the significant genes with the highest temporal variance during organ development (mean of 5.6-fold difference; range, 2.1-fold to 237.9-fold; $n = 2,000$).

Hierarchical clustering of genes with the highest variance over the developmental time course revealed several distinct profiles (Fig. 1). One pattern, composed of 371 genes, was coincident with prostate induction, in which expression peaked in E16.5 or E17.5 UGS, decreased at E18.5 and day 7, and then fell sharply through puberty and adulthood. This cluster, designated the prostate inducer profile, included secreted frizzled-related proteins 1 and 2 (*Sfrp1* and *Sfrp2*) and adult hemoglobin α and β chains (*Hba-a1* and *Hbb-b1*). Secreted frizzled-related proteins are a class of Wnt pathway inhibitors that modulate Wnt signaling through direct binding to Wnt ligands as well as binding to frizzled receptors (16). Sfrp1 promotes prostate growth and branching morphogenesis in cultures of rat neonatal ventral prostate and stimulates the growth of immortalized human prostate epithelium (17). To our knowledge, the functional role of Sfrp2 in prostate induction has not been characterized. Hba-a1 and Hbb-b1 encode the major hemoglobins of adult erythroid cells. Embryonic forms of hemoglobin (Hba-x, Hbb-y, and Hbb-z) were detectable at extremely low levels in UGS before prostate budding and not expressed at subsequent time points (data not shown). The expression of hemoglobin genes in nonerythroid tissue was unexpected but not unprecedented (18). Of interest, a transgenic mouse model designed to study erythroleukemia using fetal γ-globin or β-globin promoters to

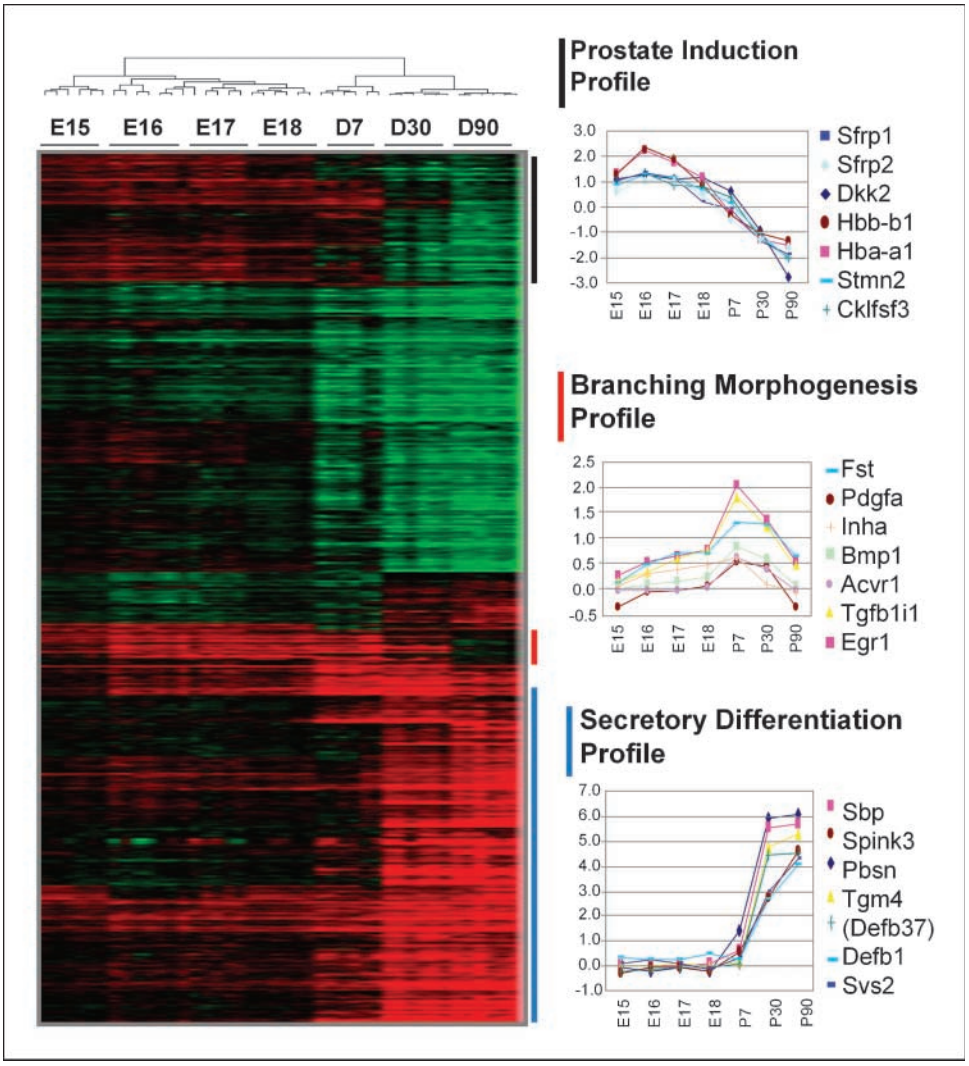

Figure 1. Gene expression programs across temporal stages of prostate development. Hierarchical clustering of the 2,000 unique genes with the highest temporal variance across mouse prostate development is depicted as a heat map in which red indicates higher expression relative to E14.5 UGS and green indicates lower expression. E15.5, E16.5, E17.5, and E18.5 are samples of embryonic UGS, whereas days 7, 30, and 90 are of postnatal prostate. Cluster dendrograms show that repeated samples from the same time point cluster together, excepting that the closely related time points of E16.5 and E17.5 UGS are not distinguished. The prostate inducer profile, branching morphogenesis profile, and secretory differentiation profile are identified to the right of the heat map with a black, red, and turquoise bar, respectively. Examples of specific genes exhibiting these profiles are given as HUGO identifiers along with plots of their behavior over the time course. The *Y* axes are $\log_2$ ratios relative to E14.5 UGS.

drive SV40T antigen was unexpectedly found to develop prostate carcinoma (19).

To validate the temporal profile of Sfrp1, Sfrp2, Hba-a1, and Hbb-b1 expression, we performed quantitative RT-PCR at each of the seven time points, producing results that were highly concordant with the microarray measurements (Supplementary Fig. S2). Immunoblots with antiserum recognizing adult hemoglobins confirmed high protein levels at E16.5 with a rapid decline over subsequent time points (Supplementary Fig. S3), and immunofluorescence localized hemoglobin protein expression to the UGS mesenchyme, with no evidence of expression in the epithelial cells of the developing prostate (Supplementary Fig. S4).

We expected genes associated with branching morphogenesis to increase expression levels after prostate induction (E17.5), peak at day 7, and fall during puberty and adulthood. Of the most variant genes, 108 (5.4%) strongly fit this profile, including *platelet-derived growth factor α* (*Pdgfa*), *follistatin* (*Fst*), *bone morphogenetic protein 1* (*Bmp1*), *inhibin α* (*Inha*), *activin A receptor type II–like 1* (*Acvr1*), and *TGFβ receptor 3* (*Tgfbr3*; Fig. 1). *Bmp1* and *Inha* are secreted morphogens in the TGFβ superfamily, whereas *Fst* is a secreted inhibitor of the TGFβ family member activin A. The high representation of ligands (Bmp1, Inha, and Fst) and receptors (Acvr1 and *Tgfbr3*) that modulate TGFβ signaling suggests a role for the TGFβ pathway specifically in prostate development. This is supported by evidence that TGFβ, activin A, and Fst each influence prostate branching morphogenesis in neonatal rodent ventral prostate cultures (20, 21).

The third profile we examined were genes associated with terminal secretory differentiation. The mouse prostate begins to produce secretory proteins that contribute to the seminal fluid just before puberty, at ~30 days postnatal. We expected these genes to exhibit low or absent expression at early time points, rise at ~day 30, and remain high after maturity (22). Three hundred and forty-two of the temporally variable genes in our analysis fit this profile (Fig. 1). All of the known mouse prostate secretory proteins were present in this group, including probasin (*Pbsn*), spermine-binding protein (*Sbp*), serine protease inhibitor Kazal type 3 (*Spink3*), transglutaminase 4 (*Tgm4*), seminal vesicle secretion 2 (*Svs2*), and prostate β defensin 1 (*Pbd1/Defb37*).

A previous report by Abbott and colleagues (15) used abundance measurements of expressed sequence tags determined from developmental stage-specific cDNA libraries to identify 285 genes altered during mouse prostate genesis. Of these genes, 192 were present on the microarrays used in the present study. We compared

the "virtual" expression analysis of these genes with transcript levels measured by microarray hybridization over roughly the same time course. Hierarchical clustering revealed concordance between the previous *in silico* analysis and the microarray results, with most genes exhibiting qualitatively similar temporal profiles (data not shown).

Gene functions associated with specific stages of mouse prostate development. To determine how developmental shifts in mouse prostate gene expression correlate with biological function, we mapped GO identifiers for biological processes, molecular functions, and cellular components onto genes represented on the mouse prostate microarray. We used a Bayesian model that incorporates uncertainty associated with microarray normalization and gene classification to assess the probability of functional enrichment (23). We confined our analysis to GO terms that were represented by at least 15 genes to ensure that functional conclusions were not drawn from categories with little overall representation. We found that several broad functional classes, such as morphogenesis (GO:0009653), cell communication (GO:0007154), and cell proliferation (GO:0008283), were active at earlier time points ($P > 0.9$), whereas immune response (GO:0006955) and transporter activity (GO:0005215) were enriched in puberty and adulthood.

To examine functional activities specifically associated with prostate induction, branching morphogenesis, and secretory differentiation, we estimated the proportion of up-regulated genes assigned a GO term at each time point and compared this with the proportion on the microarray as a whole. Hierarchical clustering of 422 GO categories revealed functions that closely followed the prostate inducer and branching morphogenesis profile, but surprisingly, no functions strongly fit the secretory differentiation profile (Supplementary Fig. S1). Although many GO categories peaked at days 30 or 90, most of these also exhibited a second minor peak at E16.5 or E17.5 (Supplementary Fig. S1). Functions associated with the prostate inducer profile included cell-cell signaling (GO:0007267), cell-cell adhesion (GO:0016337), cell cycle (GO:0007049), and the Wnt signaling pathway (GO:0016055; Supplementary Fig. S1). In addition to Sfrp1 and Sfrp2, we found that expression of Wnt2, Wnt4, Wnt5a, Dkk2, and 13 other Wnt pathway components (out of 33 genes on the array annotated to GO:0016055) followed the prostate inducer profile. The cell-matrix adhesion (GO:0007160) and integrin-mediated signaling (GO:0007229) closely followed the branching morphogenesis profile. Integrin signaling is crucial for ductal branching morphogenesis and several integrins are developmentally regulated (24, 25). We found that integrins α3, α4, α6, α7, β1, β4, and β6 as well as integrin-linked kinase and RhoA peaked in expression at postnatal day 7, during the time of active branching morphogenesis. Taken together, these analyses suggest involvement of the Wnt pathway in prostate induction, whereas integrins and TGFβ signaling may play a more prominent role in branching morphogenesis.

Genetically engineered mouse models of prostate cancer share molecular features with early prostate development. It has been proposed that common mechanisms are shared between development and cancer in which neoplastic lesions recapitulate the events of normal development in reverse, progressing from a differentiated to a dedifferentiated state (26). Importantly, key features of organogenesis involve cellular characteristics that are also hallmarks of neoplasia. In this context, expression profiling of mouse cerebellum, lung, and colon has revealed strong organ-specific connections between developmental programs and cancers arising in these tissues at a genome-wide level (14, 27). To explore relationships between prostate development and neoplasia, we evaluated two well-characterized genetically engineered mouse models of prostate carcinogenesis, a prostate-specific deletion of the *Pten* tumor suppressor gene (11), and a prostate-specific overexpression of the *Myc* oncogene (12). Mice with homozygous deletions of *Pten* develop invasive prostate cancer by 9 weeks of age. A previous study using microarray-based quantitation of gene expression in $Pten^{-/-}$ tumors identified 285 up-regulated and 241 down-regulated genes (≥2-fold difference; FDR ≤ 15%) compared with normal prostates from litter-matched controls (11). To determine relationships between genes regulated during prostate oncogenesis and the developmental phases of the prostate, we examined the behavior of the 526 $Pten^{-/-}$ tumor-associated genes over the prostate development time course by PCA using an approach described by Kho and colleagues (14). In normal development, the dominant overall trend involved genes expressed highly at either end of the developmental spectrum. This pattern was reflected by the first temporal PC (PC1), where those genes expressed at high levels early in development and subsequently monotonically decrease to low levels at prostate maturity receive a negative first PC (PC1 < 0) and genes expressed at low levels in embryogenesis and high levels at maturity comprise a positive first PC (PC1 > 0). Using the convention of Kho and colleagues, we labeled genes with negative PC1 values the prostate early mouse partition (PEMP) and the cohort with positive PC1 values the prostate late mouse partition (PLMP; Fig. 2*A*). Of the up-regulated genes in $Pten^{-/-}$ tumors, 143 (50.1%) mapped to negative PC1 coordinates, partitioning according to early prostate development, and 142 (49.9%) mapped to positive PC1 locations. Among the 241 genes down-regulated in $Pten^{-/-}$ tumors, 32 (13.3%) segregated according to the PEMP and 209 (86.7%) with late development PLMP (Fig. 2*B*). To address how many genes we would expect to segregate to early or late development by chance alone, we selected 526 genes from the developmental time course at random and performed PCA analysis. Repeated random samples of 526 genes showed that 44.3% and 55.7% segregated to early and late development, respectively. Therefore, more PEMP genes are expressed highly in $Pten^{-/-}$ tumors than expected by chance (50.1% compared with 44.3%) and more PLMP genes are down-regulated (86.7% compared with 55.7%). Hypothesis testing for equality of proportions revealed that the enrichment of both the up-regulated $Pten^{-/-}$ tumor genes in the expression program of early prostate development and down-regulated genes in late development was highly statistically significant ($P < 10^{-5}$). The odds ratio of an up-regulated Pten tumor gene segregating with early development was 6.6 (95% confidence interval, 4.2–10.2; $P < 10^{-5}$, χ^2).

To investigate if the association we observed between prostate cancer and prostate development is generalizable, we analyzed a second model of prostate carcinogenesis generated by overexpressing the Myc oncogene in prostate epithelium. Microarray-based expression profiling studies of Myc-overexpressing prostate tumors were previously reported (12), and we identified 165 differentially expressed genes (≥2-fold differential expression; FDR ≤ 15%) from this study with corresponding features in our developmental time course experiments. PCA analysis of the behavior of these genes in the developmental time course revealed that 74.2% (49 of 66) of Myc up-regulated genes segregated to early development, whereas 87.9% (87 of 99) of Myc down-regulated

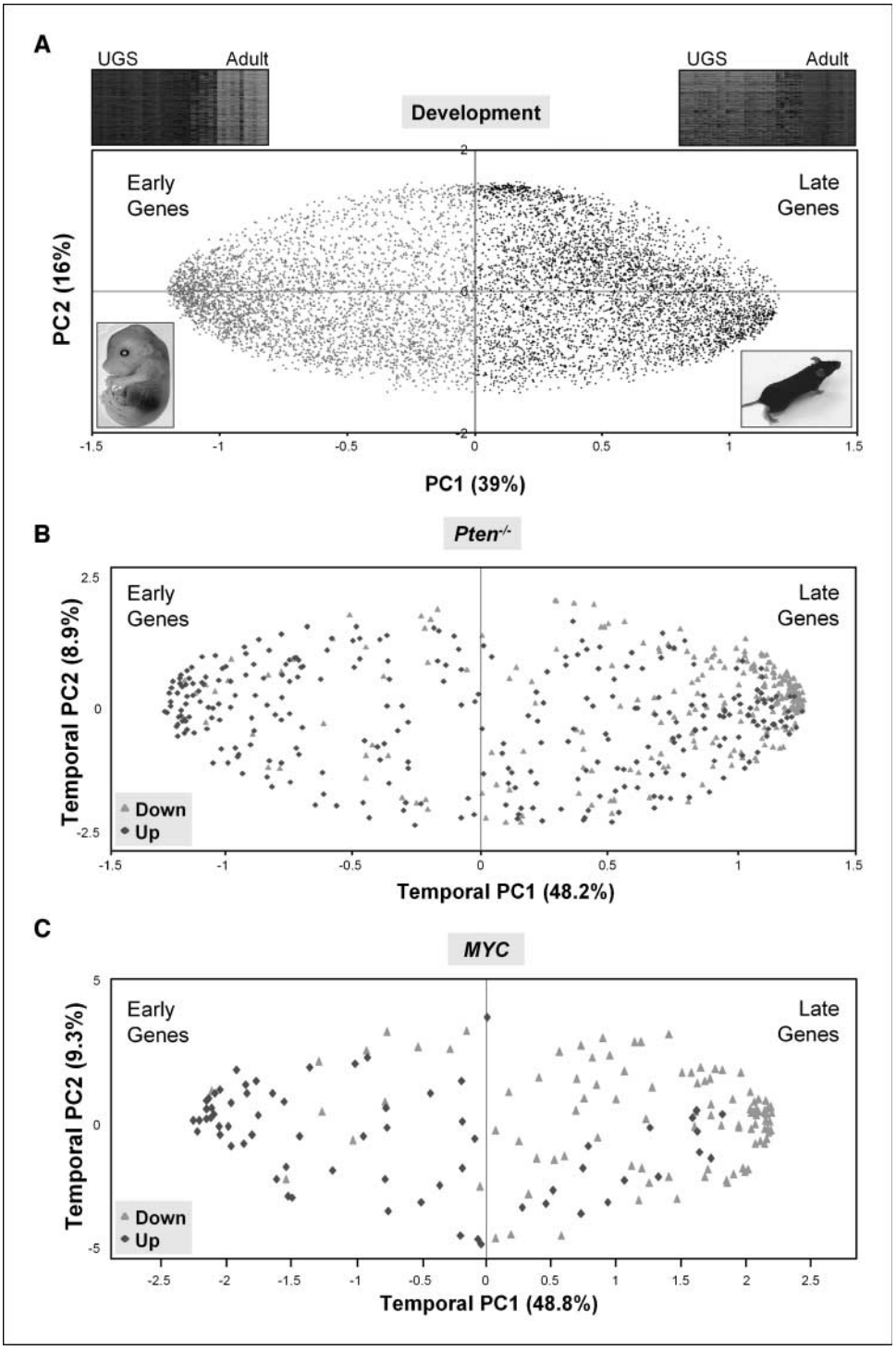

Figure 2. Gene expression maps associating prostate cancer and early development. *A,* an "egg plot" depicts the 7,993 genes expressed over the developmental time course plotted according to PC1 and PC2, where PC1 captures 39% of the variance. Genes with a negative PC1 tend to steadily increase over developmental time (early genes, *gray dots*), whereas genes with a positive PC1 tend to steadily increase over the time course (late genes, *black dots*). For comparison, heat maps depict the developmental behavior of the early genes (with the most negative PC1), and the late genes (with the most positive PC1) above the corresponding dots on the plot, where dark indicates greater relative expression and light indicates lower expression. The seven time points are ordered on the heat maps from E15.5 on the left through adult on the right (E15.5 UGS, E16.5 UGS, E17.5 UGS, E18.5 UGS, day 7 prostate, day 30 prostate, and day 90 prostate). *B,* prostate developmental expression profile of 562 genes that are regulated 2-fold (FDR < 15%) in *Pten*-null tumors compared with wild-type tissue. *Gray triangles, Pten* down-regulated genes; *black circles,* up-regulated genes. *C,* prostate developmental expression profile of 165 genes that are regulated 2-fold (FDR < 15%) in prostates overexpressing Myc compared with wild-type tissue. *Gray triangles,* Myc down-regulated genes; *black circles,* up-regulated genes. Note the correlation of prostate cancer up-regulated genes (*black circles*) with early developmental genes and cancer down-regulated genes (*gray triangles*) with late developmental genes.

genes were associated with late development (Fig. 2*C*). Proportions testing indicated that these enrichments were highly significant ($P < 10^{-5}$). The odds ratio for Myc up-regulated genes being associated with early prostate development was 20.9 (95% confidence interval, 9.2–47.3; $P < 10^{-5}$, χ^2).

To determine if the association between prostate cancer gene expression and aspects of normal organogenesis simply represents a generic developmental profile, rather than organ-specific developmental states, we analyzed the prostate cancer expression signatures in the context of a temporal gene expression profile of mouse lung development, an organ system that also involves branching morphogenesis (28). Using the PCA used for the prostate studies, we found no significant associations with stages of lung morphogenesis.

Genes altered in murine prostate adenocarcinoma map to the branching morphogenesis stage of prostate development. We next sought to place the cellular phenotype of neoplastic prostate epithelium, represented by its molecular program of

expressed genes, on the continuum of prostate development. We first specifically evaluated associations between Pten$^{-/-}$ and Myc cancer profiles with the induction, branching morphogenesis, and secretory differentiation profiles by comparing the proportion of developmental profile-related genes that received positive *t* statistics (up-regulated) in the tumors to the expected proportion based on the number of genes with positive *t* statistics in the entire data set. The prostate inducer profile was significantly enriched in the Pten$^{-/-}$ tumors but not in the Myc-driven tumors [*Pten*$^{-/-}$: 193 of 294 (65.6%) genes up-regulated, $P < 0.00001$, proportions test; Myc: 113 of 193 (58.5%) genes up-regulated, $P = 0.27$, proportions test]. The branching morphogenesis profile was strongly enriched in both the *Pten*$^{-/-}$ and Myc-driven cancers [*Pten*: 72 of 91 (79.1%) genes up-regulated, $P < 0.00001$, proportions test; *Myc*: 49 of 64 (76.6%) genes up-regulated, $P < 0.0005$, proportions test]. Conversely, over 70% of genes associated with the secretory differentiation profile were down-regulated in both *Pten*-null and Myc-driven cancers. We next projected the expression profiles generated from individual Myc or *Pten*$^{-/-}$ tumors onto the genomic developmental trajectory of the mouse prostate represented by PCs (Fig. 3*A*). Pten tumors localized in a tight cluster between P7 and P30, whereas Myc tumors were more dispersed over developmental space slightly preceding and slightly following postnatal day 7 (Fig. 3*B*), a finding that may reflect the pleiotropic activities attributable to the Myc protein (29). We are not aware of any morphologic features differing between these models that would account for their placement on the developmental time course. Together, these results are concordant with our findings that up-regulated and down-regulated genes in murine prostate cancer segregate with early and late development, respectively. In addition, these data suggest that genes comprising the branching morphogenesis profile may contribute to processes influencing carcinogenesis.

Genes comprising the branching morphogenesis program are altered in human prostate carcinoma. The complex developmental process of branching morphogenesis involves several features that are also operative in invasive prostate cancers. These include cellular processes contributing to cell movement, adhesion, invasion, division, and death that are extensively influenced through interactions with surrounding mesenchyme and extracellular matrix. To determine if genes operative in the normal branching morphogenesis program exhibit elevated activity in human prostate cancers, we evaluated transcript abundance levels of orthologous human genes measured by microarray-based profiling studies of human tumors. These comprised two studies, True and colleagues (30) and Tomlins and colleagues (31), where microdissected epithelium was acquired, and one study reported by Lapointe and colleagues (32) that used macrodissected tissue samples. Overall, in each data set, ~20% of the genes comprising the murine branching morphogenesis program were found to be statistically increased in human prostate cancers relative to benign tissue. Although the gene representation varied across studies, in a large part due to different probes present on the different microarray platforms, several genes exhibited significant increases in prostate cancers consistently including *peroxiredoxin 4* (*PRDX4*), *SLC43A1/POV1*, and the *DNA (cytosine-5-)-methyltransferase 3α* (*DNMT3A*; Fig. 4). Importantly, many of the genes comprising the branching morphogenesis network have not been extensively studied in the context of prostate neoplasia.

We next sought to determine if genes associated with branching morphogenesis were associated with malignant tumor characteristics. We evaluated a data set reported by Stephenson and colleagues (33) that used microarrays to profile transcript levels in prostate tumors from 79 patients with attendant clinical follow-up delineating biochemical relapse after radical prostatectomy. Of the 91 genes comprising the BMP, 84 had orthologs represented in this data set. A single estimate of the expression level in each sample was generated and the association between PSA relapse and transcript levels was determined by logistic regression. We found

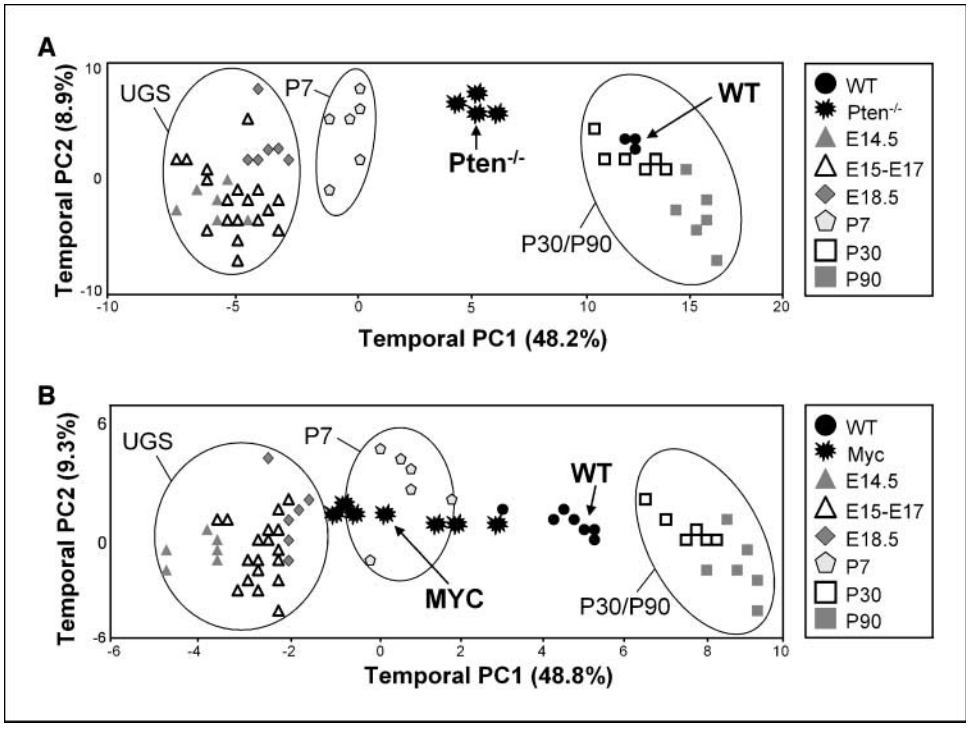

Figure 3. Localization of Pten$^{-/-}$ and Myc-driven prostate cancers to the branching morphogenesis stage (*P7*) of prostate development. The seven prostate developmental time points are separated by PCA analysis according to temporal PC1 and PC2, where PC1 represented ~50% of the variance. Individual *Pten*$^{-/-}$ (*A*) and *Myc*-overexpressing (*B*) tumors are projected onto the backdrop of development. Note that both *Pten*$^{-/-}$ and *Myc*-driven tumors cluster in the early postnatal period, closest to postnatal day 7 during branching morphogenesis.

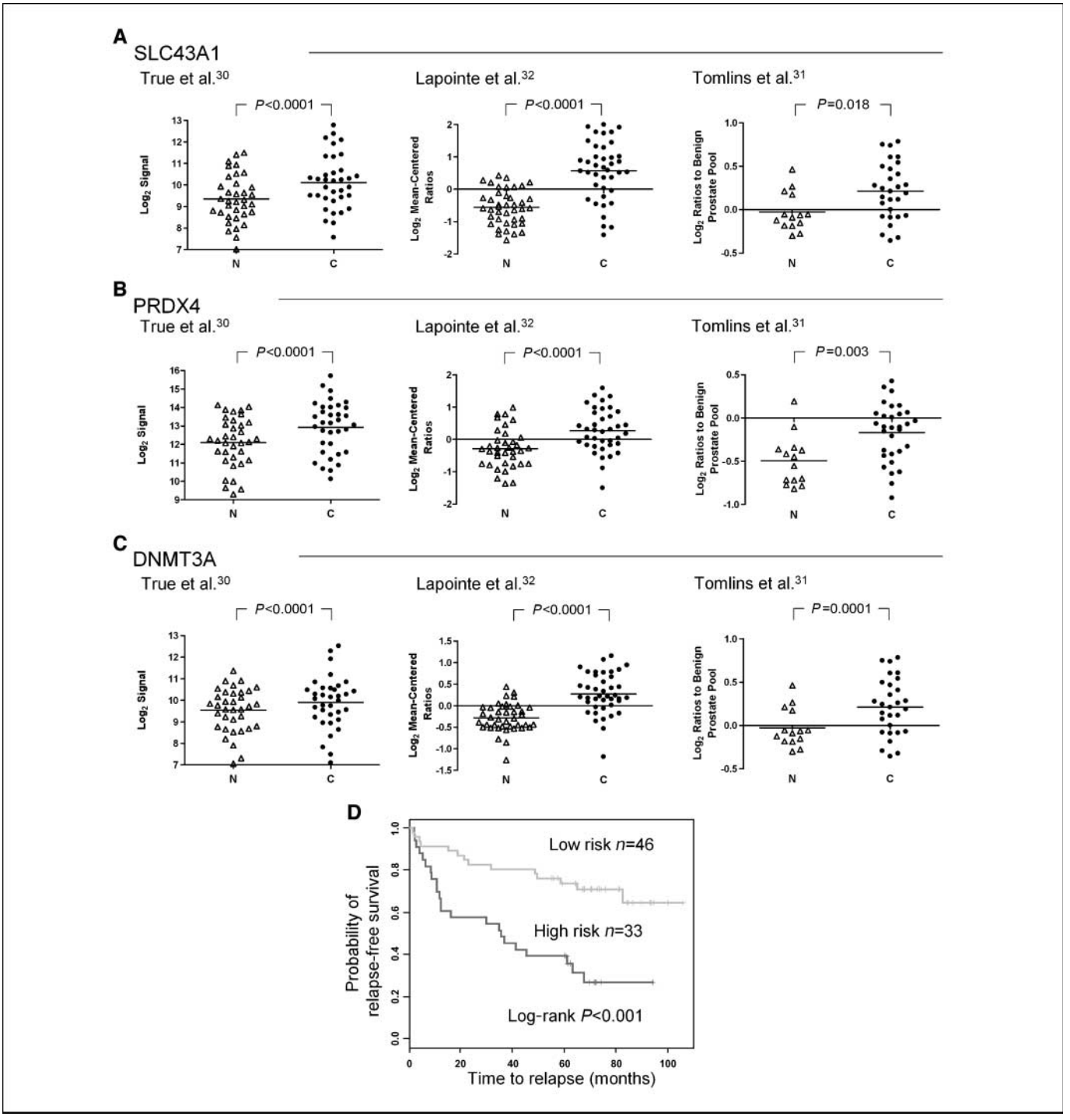

Figure 4. Genes comprising the branching morphogenesis signature are dysregulated in human prostate cancer and associate with outcome. Microarray-based measurements of SLC43A1 (*A*), PRDX4 (*B*), and DNMT3A (*C*) transcript abundance levels between normal (*N*; *circles*) and cancerous (*C*) epithelium (*triangles*) are plotted from three independent data sets. For True and colleagues data ($n = 35$), differences between normal and cancer were assessed by paired, two-sample *t* test of $\log_2$-transformed signal values. For Lapointe and colleagues data ($n = 41$), differences between normal and cancer were assessed by paired, two-sample *t* test of $\log_2$-transformed ratios to cell line control. For Tomlins and colleagues data ($n = 31$), differences between normal and cancer were assessed by unpaired, two-sample *t* test of $\log_2$-transformed ratios to benign prostate pool. *D,* a 14-gene signature associated with branching morphogenesis was used to classify prostate cancer samples by disease recurrence as determined by PSA relapse. The difference in disease-free survival, defined as no PSA relapse >0.1 in any follow-up time point, for the two groups was quantified using the survDiff function in R and the *P* value was reported by log-rank test.

that 14 genes were significantly associated with disease relapse ($P \leq 0.05$) and a classifier using this gene signature provided discriminatory outcome information associating with disease recurrence ($\chi^2 = 14.4$; $P < 0.001$; Fig. 4). Further confirmation of the independent predictive power of genes comprising the branching morphogenesis profile will require a directed study with long-term clinical outcomes that incorporates other risk factors associated with tumor behavior.

Discussion

Carcinomas arising in a diverse range of organs and cell types are known to display immature features and are accompanied by marked changes in gene expression (34). A subset of genes aberrantly expressed in tumor cells is known to normally exhibit highly compartmentalized spatial and temporal expression patterns localized to specific stages of embryonic development (9, 35). Several embryonic proteins, such as carcinoembryonic antigen and α-fetoprotein, have been developed into useful diagnostic tumor markers. However, with few exceptions, the overall relationships between tumors and developmental programs defined at the genetic level have not been evaluated (14, 27). In this study, we sought to determine molecular features underlying events linked to normal developmental processes in the prostate gland and those accompanying neoplastic transformation. Overall, we identified significant correlations between gene expression profiles representing early stages of prostate organogenesis and two distinct mouse models of prostate carcinoma arising in the context of *Pten* loss or *Myc* overexpression. In general, transcripts differentially up-regulated in carcinomas were more likely to also be expressed early in development and decline with progressive organ maturation, whereas genes expressed highly in the mature differentiated prostate gland were down-regulated in carcinomas. Similar overall trends were observed in studies comparing gut development and colorectal tumors (27) and of cerebellar development and medulloblastomas (14). Together, these studies provide strong support for a general reactivation of primitive cellular programs operating to govern a range of phenotypic opportunities involving cell position, division, motility, and invasion that are provided by intrinsic and extrinsic cues.

The molecular profiles derived from prostate cancers exhibited the greatest association with the branching morphogenesis stage of prostate development. The process of branching morphogenesis involves a complex interplay of cellular events that in many ways recapitulates features of malignant cells (36). The process is critical for the formation of arborized organs that span the development of tracheal networks in insects to a diverse array of human tissues that include the pancreas, lung, salivary gland, kidney, breast, and prostate (6, 37). Branching morphogenesis entails reorganization of epithelial tissues to form complex but highly structured tubular assemblies that function to produce and transport fluids and gases over large surface areas (36). A series of sequential and often iterative biochemical and biomechanical steps are required for the proper construction of the networks, and many of the key molecular features governing these processes have been elucidated. A critical component of the process involves the invagination and subsequent invasion of epithelial buds and outgrowths into surrounding mesenchyme. Importantly, the incursion of epithelium is highly dependent on signals derived from the surrounding stroma, an attribute increasingly recognized to play an important role in carcinogenesis. Key regulators of these processes include FGF10, Shh, Bmp4, TGFβ, as well as members of the matrix metalloproteinase, a disintegrin and metalloproteinase, and serine protease families (38, 39). The matrix metalloproteinases are of particular interest due to their integral roles in regulating epithelial-mesenchymal cross-talk and their influence on migratory processes through proteolysis of matrix molecules and the generation of motogens such as laminin-5 fragments (40). The leading edge of migrating epithelial cells has been shown to exhibit mesenchymal phenotypes, allowing for penetration through matrix and stromal cell tissue constituents, a process also well described in the context of tumor cell epithelium to mesenchymal transition (41, 42). Thus, tumors exhibiting transcript profiles congruent with a branching morphogenesis developmental stage might be expected to exhibit characteristics of enhanced invasion, metastasis, and early relapse after surgical resection.

The comparative profiling studies we report here identified several genes that have not been extensively studied in the context of normal developmental processes or prostate carcinoma. *PRDX4* is a member of a multifunctional antioxidant protein family that primarily serves to provide cellular protection against oxidative stress (43). Peroxiredoxin family members also regulate proliferation, in part through intracellular signaling cascades that apply hydrogen peroxide as a molecular second messenger. No known roles for *PRDX4* have been described in the context of development, although other peroxiredoxin family members interact with the androgen receptor (AR) and modulate AR-mediated signaling (44). All of the prostate cancer studies we evaluated showed elevated expression of PRDX4 in neoplastic lesions. *DNMT3A* encodes an enzyme involved in *de novo* methylation of genomic DNA, a critical step for regulating genomic imprinting and X-chromosome inactivation. Prior studies have shown aberrant *de novo* methylation of growth-regulatory genes in human tumorigenesis (45). To date, no specific role for *DNMT3A* has been shown for genitourinary tract developmental processes, although a myriad of developmental abnormalities results from deleting *Dnmt3a* in mouse models and conditional *Dnmt3a* mutant males show impaired spermatogenesis (46). Studies in prostate cancer have shown increased *Dnmt3a* expression in tumors developing in the TRAMP model (47), and increased *DNMT3A* expression has been associated with progression to androgen-independent growth *in vitro* (47, 48). *SLC43A1* encodes a protein that functions in the sodium-independent transport of neutral amino acids. *SLC43A1* was originally identified as a transcript up-regulated in a clinically aggressive prostate cancer and designated *POV1* (49). To date, there are no studies showing a mechanistic role for *SLC43A1* in developmental processes.

In summary, global assessments of gene use in prostate cancers and normal development provide intriguing links between the two processes. This perspective allows for the identification of specific genes as well as regulatory patterns, pathways, and networks that operate to direct the complex processes required for both the homeostasis and evolution of normal and malignant tissues. Exploiting normal developmental systems may provide a convenient and tractable model to study mechanisms that play influential roles in invasive neoplastic growth.

Disclosure of Potential Conflicts of Interest

No potential conflicts of interest were disclosed.

Acknowledgments

Received 12/27/2007; revised 11/19/2008; accepted 11/24/2008; published OnlineFirst 02/17/2009.

Grant support: NIH grants U01CA84294, U54CA126540, R01DK069690, R01DK63919, and P20RR016472 and Department of Defense grants PC041158 and PC060595.

The costs of publication of this article were defrayed in part by the payment of page charges. This article must therefore be hereby marked *advertisement* in accordance with 18 U.S.C. Section 1734 solely to indicate this fact.

We thank Dr. Matthew Fero, Norman Greenberg, and members of the Nelson laboratory for helpful advice.

References

1. Potter JD. Morphostats: a missing concept in cancer biology. Cancer Epidemiol Biomarkers Prev 2001;10: 161–70.
2. Howard B, Ashworth A. Signalling pathways implicated in early mammary gland morphogenesis and breast cancer. PLoS Genet 2006;2:e112.
3. Peifer M, McEwen DG. The ballet of morphogenesis: unveiling the hidden choreographers. Cell 2002;109:271–4.
4. Hanahan D, Weinberg RA. The hallmarks of cancer. Cell 2000;100:57–70.
5. Cunha GR, Ricke W, Thomson A, et al. Hormonal, cellular, and molecular regulation of normal and neoplastic prostatic development. J Steroid Biochem Mol Biol 2004;92:221–36.
6. Thomson AA, Marker PC. Branching morphogenesis in the prostate gland and seminal vesicles. Differentiation 2006;74:382–92.
7. Fan L, Pepicelli CV, Dibble CC, et al. Hedgehog signaling promotes prostate xenograft tumor growth. Endocrinology 2004;145:3961–70.
8. Karhadkar SS, Bova GS, Abdallah N, et al. Hedgehog signalling in prostate regeneration, neoplasia and metastasis. Nature 2004;431:707–12.
9. Shou J, Ross S, Koeppen H, de Sauvage FJ, Gao WQ. Dynamics of notch expression during murine prostate development and tumorigenesis. Cancer Res 2001;61: 7291–7.
10. Bianchi-Frias D, Pritchard C, Mecham BH, Coleman IM, Nelson PS. Genetic background influences murine prostate gene expression: implications for cancer phenotypes. Genome Biol 2007;8:R117.
11. Wang S, Gao J, Lei Q, et al. Prostate-specific deletion of the murine Pten tumor suppressor gene leads to metastatic prostate cancer. Cancer Cell 2003;4:209–21.
12. Ellwood-Yen K, Graeber TG, Wongvipat J, et al. Myc-driven murine prostate cancer shares molecular features with human prostate tumors. Cancer Cell 2003;4:223–38.
13. Tusher VG, Tibshirani R, Chu G. Significance analysis of microarrays applied to the ionizing radiation response. Proc Natl Acad Sci U S A 2001;98:5116–21.
14. Kho AT, Zhao Q, Cai Z, et al. Conserved mechanisms across development and tumorigenesis revealed by a mouse development perspective of human cancers. Genes Dev 2004;18:629–40.
15. Abbott DE, Pritchard C, Clegg NJ, et al. Expressed sequence tag profiling identifies developmental and anatomic partitioning of gene expression in the mouse prostate. Genome Biol 2003;4:R79.
16. Jones SE, Jomary C. Secreted Frizzled-related proteins: searching for relationships and patterns. BioEssays 2002;24:811–20.
17. Joesting MS, Perrin S, Elenbaas B, et al. Identification of SFRP1 as a candidate mediator of stromal-to-epithelial signaling in prostate cancer. Cancer Res 2005;65:10423–30.
18. Liu L, Zeng M, Stamler JS. Hemoglobin induction in mouse macrophages. Proc Natl Acad Sci U S A 1999;96: 6643–7.
19. Perez-Stable C, Altman NH, Brown J, Harbison M, Cray C, Roos BA. Prostate, adrenocortical, and brown adipose tumors in fetal globin/T antigen transgenic mice. Lab Invest 1996;74:363–73.
20. Cunha GR, Foster B, Thomson A, et al. Growth factors as mediators of androgen action during the development of the male urogenital tract. World J Urol 1995;13:264–76.
21. Cancilla B, Jarred RA, Wang H, Mellor SL, Cunha GR, Risbridger GP. Regulation of prostate branching morphogenesis by activin A and follistatin. Dev Biol 2001; 237:145–58.
22. Aumuller G, Seitz J. Protein secretion and secretory processes in male accessory sex glands. Int Rev Cytol 1990;121:127–231.
23. Bhattacharjee M, Pritchard CC, Nelson PS, Arjas E. Bayesian integrated functional analysis of microarray data. Bioinformatics 2004;20:2943–53.
24. De Arcangelis A, Georges-Labouesse E. Integrin and ECM functions: roles in vertebrate development. Trends Genet 2000;16:389–95.
25. Danen EH, Sonnenberg A. Integrins in regulation of tissue development and function. J Pathol 2003;201: 632–41.
26. Edwards PA. The impact of developmental biology on cancer research: an overview. Cancer Metastasis Rev 1999;18:175–80.
27. Lepourcelet M, Tou L, Cai L, et al. Insights into developmental mechanisms and cancers in the mammalian intestine derived from serial analysis of gene expression and study of the hepatoma-derived growth factor (HDGF). Development 2005;132:415–27.
28. Mariani TJ, Reed JJ, Shapiro SD. Expression profiling of the developing mouse lung: insights into the establishment of the extracellular matrix. Am J Respir Cell Mol Biol 2002;26:541–8.
29. Orian A, van Steensel B, Delrow J, et al. Genomic binding by the *Drosophila* Myc, Max, Mad/Mnt transcription factor network. Genes Dev 2003;17:1101–14.
30. True L, Coleman I, Hawley S, et al. A molecular correlate to the Gleason grading system for prostate adenocarcinoma. Proc Natl Acad Sci U S A 2006;103: 10991–6.
31. Tomlins SA, Mehra R, Rhodes DR, et al. Integrative molecular concept modeling of prostate cancer progression. Nat Genet 2007;39:41–51.
32. Lapointe J, Li C, Higgins JP, et al. Gene expression profiling identifies clinically relevant subtypes of prostate cancer. Proc Natl Acad Sci U S A 2004;101: 811–6.
33. Stephenson AJ, Smith A, Kattan MW, et al. Integration of gene expression profiling and clinical variables to predict prostate carcinoma recurrence after radical prostatectomy. Cancer 2005;104:290–8.
34. Uriel J. Cancer, retrodifferentiation, and the myth of Faust. Cancer Res 1976;36:4269–75.
35. Smalley MJ, Dale TC. Wnt signalling in mammalian development and cancer. Cancer Metastasis Rev 1999; 18:215–30.
36. Affolter M, Bellusci S, Itoh N, Shilo B, Thiery JP, Werb Z. Tube or not tube: remodeling epithelial tissues by branching morphogenesis. Dev Cell 2003;4: 11–8.
37. Lu P, Sternlicht MD, Werb Z. Comparative mechanisms of branching morphogenesis in diverse systems. J Mammary Gland Biol Neoplasia 2006;11:213–28.
38. Cardoso WV, Lu J. Regulation of early lung morphogenesis: questions, facts and controversies. Development 2006;133:1611–24.
39. Kheradmand F, Werb Z. Shedding light on sheddases: role in growth and development. BioEssays 2002;24:8–12.
40. Koshikawa N, Giannelli G, Cirulli V, Miyazaki K, Quaranta V. Role of cell surface metalloprotease MT1-MMP in epithelial cell migration over laminin-5. J Cell Biol 2000;148:615–24.
41. Thiery JP. Epithelial-mesenchymal transitions in development and pathologies. Curr Opin Cell Biol 2003;15:740–6.
42. Thiery JP. Epithelial-mesenchymal transitions in tumour progression. Nat Rev Cancer 2002;2:442–54.
43. Fujii J, Ikeda Y. Advances in our understanding of peroxiredoxin, a multifunctional, mammalian redox protein. Redox Rep 2002;7:123–30.
44. Park SY, Yu X, Ip C, Mohler JL, Bogner PN, Park YM. Peroxiredoxin 1 interacts with androgen receptor and enhances its transactivation. Cancer Res 2007;67: 9294–303.
45. Baylin SB, Herman JG, Graff JR, Vertino PM, Issa JP. Alterations in DNA methylation: a fundamental aspect of neoplasia. Adv Cancer Res 1998;72:141–96.
46. Okano M, Bell DW, Haber DA, Li E. DNA methyltransferases Dnmt3a and Dnmt3b are essential for *de novo* methylation and mammalian development. Cell 1999;99:247–57.
47. Patra SK, Patra A, Zhao H, Dahiya R. DNA methyltransferase and demethylase in human prostate cancer. Mol Carcinog 2002;33:163–71.
48. Pang ST, Weng WH, Flores-Morales A, et al. Cytogenetic and expression profiles associated with transformation to androgen-resistant prostate cancer. Prostate 2006;66:157–72.
49. Cole KA, Chuaqui RF, Katz K, et al. cDNA sequencing and analysis of POV1 (PB39): a novel gene up-regulated in prostate cancer. Genomics 1998;51:282–7.